Copyright © 2010 Tech Science Press CMC, vol.17, no.1, pp.41-57, 2010

Effects of TGO Roughness on Indentation Response of Thermal Barrier Coatings

Taotao Hu[1] and Shengping Shen[1,2]

Abstract: In this paper, an axisymmetric indentation model is set up to calculate the effects of the roughness of the thermally grown oxide (TGO) layer, which was modeled as a sinusoidal wave, on the indentation response of the thermal barrier coatings. It is found that the amplitude, wavelength, and thickness of the thermally grown oxide layer have obvious influences on the indentation response, while the effect of the indenter position can be neglected. In the top coating layer, residual stress mainly occurs below the indenter and around the nearest two peaks of the thermally grown oxide layer to the indenter. Only when the indentation depth is less than 10% of the thickness of the top coating layer, the influence of TGO roughness on the force versus displacement curves of the indentation can be ignored. Correlating this work with the experimental data from indentation test may lead to improved characterization of the mechanical properties of TBC systems.

Keywords: Thermal barrier coating; Thermally grown oxide; Indentation; Finite element analysis

1 Introduction

Thermal barrier coating (TBC) systems have been widely used in modern jet engines and gas turbines. They can protect structural materials and allow for hot gas temperatures to increase the efficiency of the engine. TBC can decrease the temperature of the metallic substrate by about 100-150 ˚C (Vaidyanathan *et al.*, 2004; Thompson and Clyne, 2001; Schlichting *et al.*, 2003) when they are applied to turbine blades made of nickel base superalloy. Hence, it is important to investigate the mechanical behaviors of the thermal barrier coatings.

The indentation test has been the standard method for material characterization. The load-displacement curve of the indentation test is regarded as the "fingerprint"

[1] MOE Key Laboratory for Strength and Vibration, School of Aerospace, Xi'an Jiaotong University, Xi 'an 710049, China

[2] Corresponding author: Tel/Fax: 86-29-82660977; E-mail: sshen@mail.xjtu.edu.cn

of a material, from which one can obtain the intrinsic material information. Moreover, it is convenient to perform and does not need to remove films from their substrates. Indentation test provides a convenient nondestructive experimental procedure for evaluating basic material properties of the thin film/substrate systems (Nix, 1989). However, in general, the indentation itself only furnishes information on hardness and Young's modulus. Furthermore, the films are supported by the substrates, thus, substrate-independent measurements of thin-film properties are complicated because of the small thickness of film, the complex deformation of the film/substrate system, and the measuring resolution of the instrument. On the other hand, the finite element method provides a numerical method to investigate complicated indentation problems. Correlation of the finite element analysis with the experimental data from indentation test may bring on improved characterization of the mechanical properties of thin films and multi-layer systems. Oliver and Pharr (1992) developed an improved technique for determining hardness and elastic-modulus by means of indentation experiments. Nix and Gao (1998) analyzed the indentation size effects in crystalline materials by employing the strain gradient plasticity. Huang and Pelegri (2003) investigated the nanoindentation response of low-k porous silica thin films spin coated on silicon substrates. Huang and Pelegri (2007) also employed the finite element method to analyze the nanoindentation with friction contact at the film/substrate interface. Guo *et al*. (2006) studied the effects of the substrate on the indentation of the coating systems by using finite element method. Up to now, most of the finite element simulations on the indentation of the multi-layer systems assume that the interface is a plane. However, in TBC and many other multi-layer systems, the interfaces actually are very complicated, and not planar. For examples, during operation, a thin thermally grown oxide (TGO) layer in TBC is formed, which is usually rough. Moreover, it is well known that the TGO layer acts crucial role in TBC systems, and controls the TBC behavior (Rabiei and Evans, 2000; He *et al*., 2003). Although TBC fails in several different ways, the mechanisms of greatest concern are those that intimately involve the growth of the TGO (Rabiei and Evans, 2000; He *et al*., 2003). Hence, in order to improve the characterization of the mechanical properties of TBC systems, it is necessary to investigate the effects of the roughness of TGO layer on the indentation response of the TBC systems by using finite element analysis, which can be correlated with the experimental data of the indentation test.

The thermally grown oxide layer is usually modeled as a sinusoidal wave (Safar *et al*., 2002; Aktaa *et al*., 2005), which can be characterized by its amplitude, wavelength, and thickness. This paper focuses on the effects of the TGO roughness including its amplitude, wavelength, and thickness on the indentation response of thermal barrier coatings by using finite element analysis. The effect of the indenter position on the indentation response is also investigated.

2 Indentation model

As shown in Fig. 1, the indenter is conical with semi-conical angle 70.3°. The indentation test using a conical indenter is a typically axisymmetric problem, which is solved by using ABAQUS (Hibbitt, 2005) in this work. The axisymmetric indentation model including the boundary conditions and aspect parameters are depicted in Fig. 1. The TBC system considered here consists of three layers, the top coatings (TC), the bonding coatings (BC) and the superalloy substrate. During operation, a thin thermally grown oxide (TGO) layer between the TC and BC is formed. Moreover, the interface between the TC and BC layers is modeled as a sinusoidal wavy interface with a wavelength λ_{TGO} and an amplitude A_{TGO} (half of max-to-min range) as shown in Fig. 1. The assumption about the sinusoidal wavy interface has been adopted and verified in many research papers on the thermal barrier coatings (e.g., Safar *et al.*, 2002; Aktaa *et al.*, 2005).

In this work, the width of the computational model is taken to be 0.6 mm, which is equivalent to at least ten times wavelength of the sinusoidal wave. Thus, the effects of the boundary on the indentation response can be neglected. The average thicknesses of the TC layer and BC layer are both 0.1 mm, and that of the substrate is 1.6 mm. The maximum indentation depth in the simulation is 0.028 mm (i.e., 28% thickness of the TC layer). In the finite element analysis, the symmetric boundary condition is applied on the left boundary, to restrict its moving along horizontal direction, and the bottom is constrained vertically.

Furthermore, the following assumptions are employed in this work for simplification:

1. The indenter is rigid, and the friction between the contact surfaces is free;
2. all layers are homogeneous and isotropic;
3. there is non-slip on the interface between TC and BC layers;
4. all layers are initially stress-free at room temperature.

3 Computational models

As shown in Fig. 2, the meshes in the TC, TGO and BC layers are fine enough to capture the deformation in these layers, while the coarsen meshes are used in the superalloy substrate. The load is enforced by controlling the vertical displacement of the indenter.

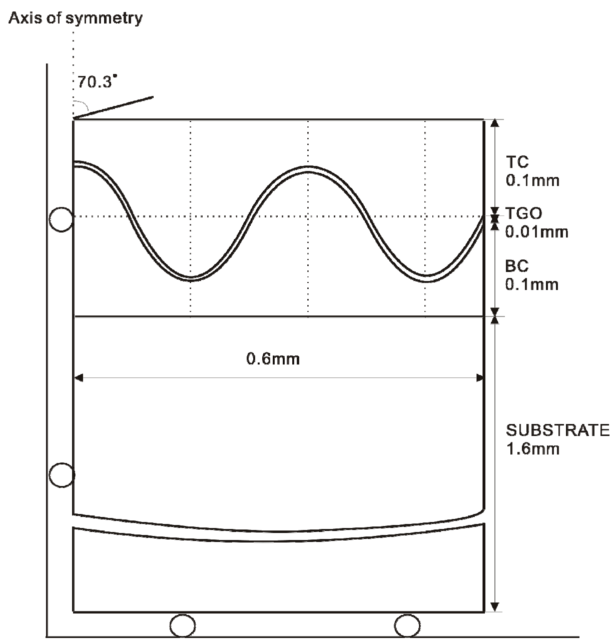

Figure 1: Schematic of the indentation model and the boundary conditions

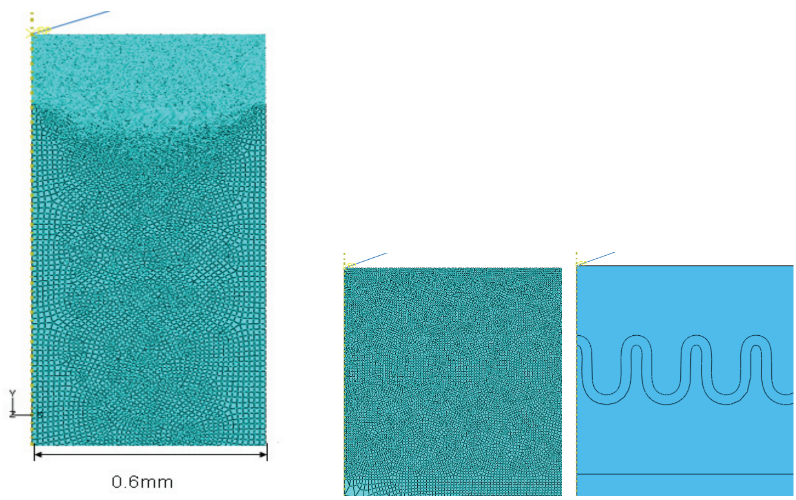

(a) Mesh pattern (b) Local enlargement around the indenter

Figure 2: Finite element model

In this simulation, the TC, TGO and BC layers are considered to be ideal elastic-plastic, and obey the von Mises yielding criterion. The superalloy substrate is assumed to be linear elastic. All the related material parameters (Guo *et al.*, 2006; He *et al.*, 2003; Safar *et al.*, 2002; Martena *et al.*, 2006) are listed in Table 1.

Table 1: Material parameters of the TBC system

	Young's modulus /MPa	Poisson ratio	Yield stress /MPa
TC	17471	0.2	2000
TGO	380000	0.27	10000
BC	182590	0.3	400
Substrate	211000	0.3	

4 Results and discussions

In this section, we will discuss the effects of the roughness of the TGO layer on the load-displacement curve of the indentation. The rigid indenter is gradually pressed into the TBC vertically in the finite element analysis, that is implemented through a number of steps during loading and unloading.

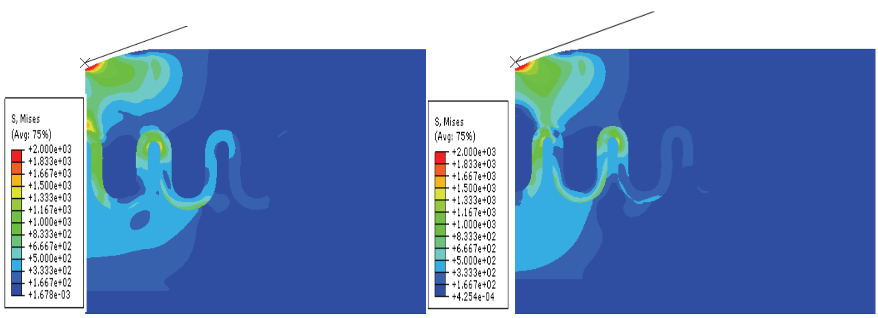

(a) wave peak (b) wave trough

Figure 3: The distribution of the residual von Mises equivalent stress in TBC for different indenter positions

4.1 *Influence of the position of indenter on indentation response*

At first, we will investigate the effect of the indenter position on the indentation response. Fig. 3(a) and 3(b) give the distribution of the residual von Mises equivalent stress after unloading for the indenter position on the point corresponding to the TGO wave crest and wave trough, respectively, with the thickness of TGO $T_{TGO} = 0.01$mm, the TGO amplitude A_{TGO}=0.03mm, and the wavelength of TGO λ_{TGO}=0.06mm. As seen, the residual stress zones in the TC layer are located just below the indenter and around the nearest two TGO wave crests to the indenter regardless of the indenter position.

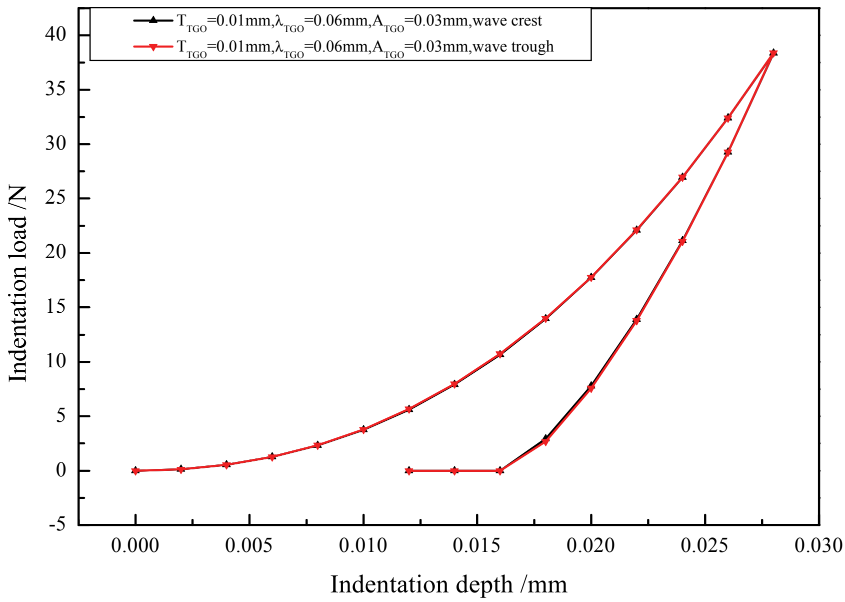

Figure 4: Force versus displacement curves for different indenter positions

Fig. 4 plots the effect of indenter position on the force versus displacement curves of the indentation for the case with $A_{TGO} = 0.03$ mm, λ_{TGO}=0.06 mm and $T_{TGO} = 0.01$ mm. It can be stated that, the effect of indenter position can be ignored since the force versus displacement curves almost completely overlap. Thus, in the followings, we only consider the cases with the indenter position on the point corresponding to the TGO wave crest.

4.2 Influence of the thickness on indentation response

Fig. 5 illustrates the distribution of the residual von Mises equivalent stress after unloading for different TGO thickness T_{TGO} with $A_{TGO} = 0.03$ mm andλ_{TGO}=0.06

mm. As seen, in the TC layer the magnitudes of the residual stresses near the indenter are almost same, though the TGO thickness T_{TGO} varies. Since the thickness of the TGO layer is very small compared to the thickness of the TC layer (only 2.5%∼10%), and the distance between the TGO and the indenter is relatively large, the effect of the TGO thickness on the residual stress near the indenter is negligible. The maximal stress in the TGO layer appears around the second nearest wave crest to the indenter, and increases with decreasing the TGO thickness. These phenomena are mainly due to the relatively large stiffness and yield strength of TGO layer.

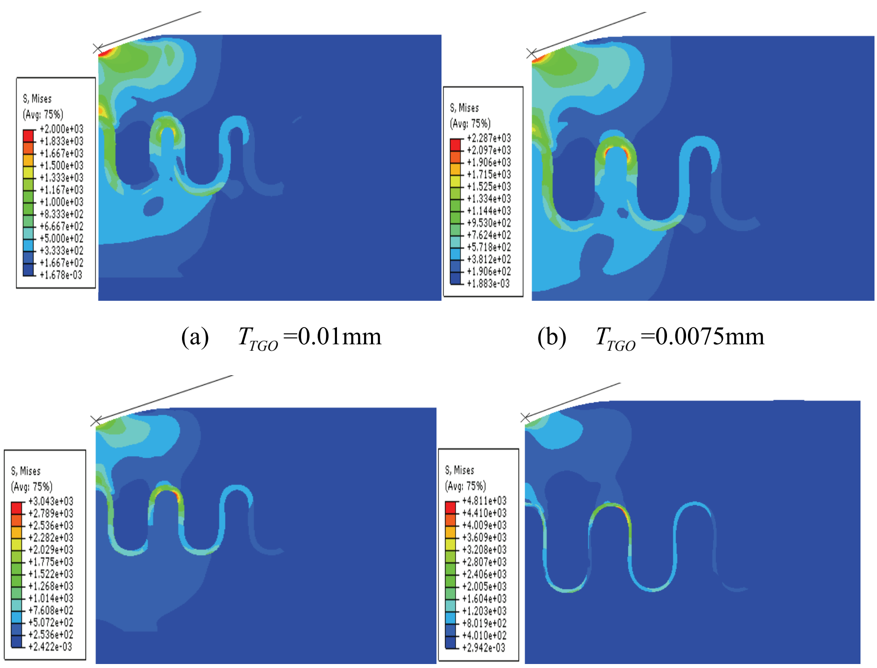

(a) T_{TGO}=0.01mm (b) T_{TGO}=0.0075mm

(c) T_{TGO}=0.005mm (d) T_{TGO}=0.0025mm

Figure 5: The distribution of the residual von Mises equivalent stress in TBC for different TGO thickness

Fig. 6 displays the effect of the TGO thickness on the force versus displacement curves of the indentation for the case with $A_{TGO} = 0.03$ mm and λ_{TGO}=0.06 mm. Fig. 7 gives a local enlargement of Fig. 6. As seen, the force versus displacement

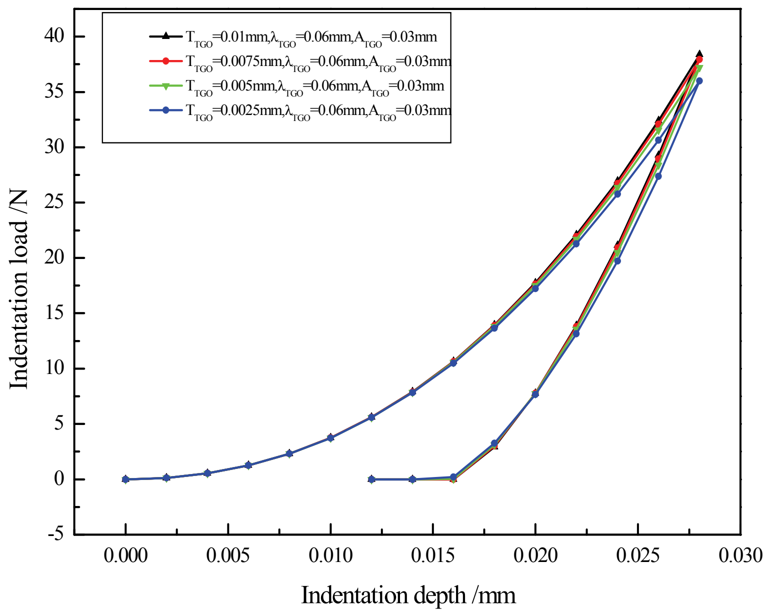

Figure 6: Force versus displacement curves for different thickness of TGO

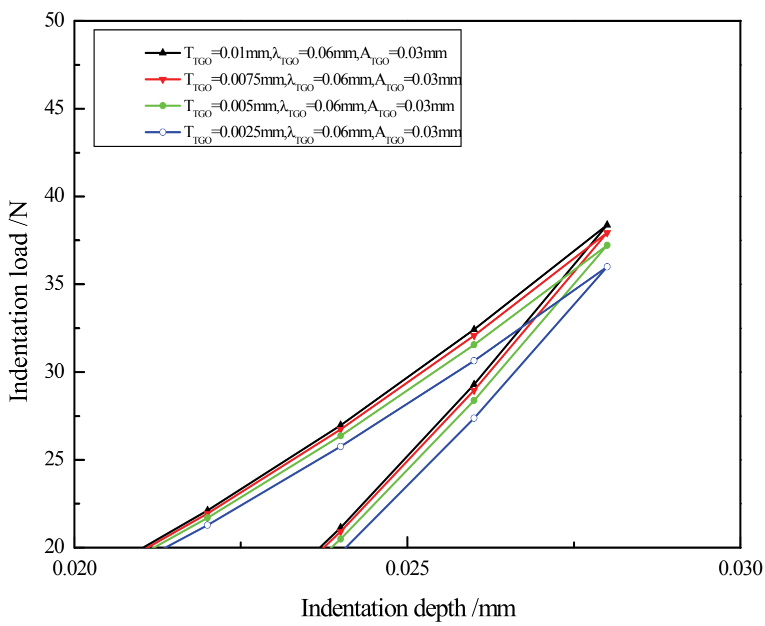

Figure 7: The local enlargement of Fig. 6

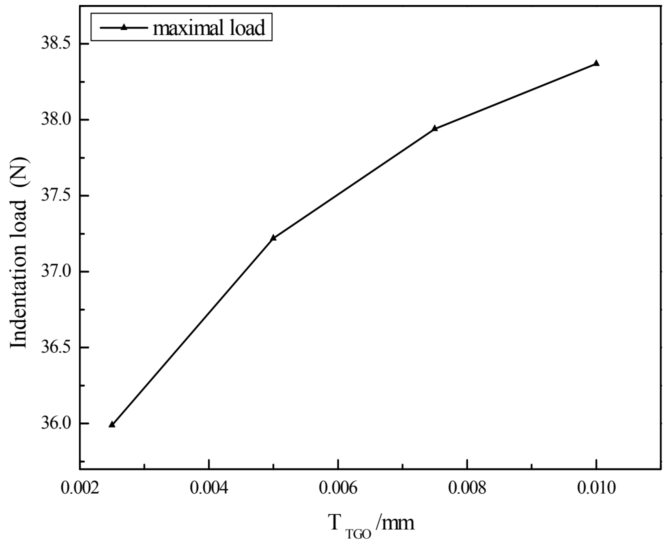

Figure 8: The variation of the maximum load with the thickness of TGO

curves do not overlap again when the depth of indentation is beyond 0.016mm (16% of the TC layer thickness). Hence, the effect of the TGO thickness is obvious. The load increases as the TGO thickness increases. Thus, one can conclude that, the thicker the TGO layer is, the harder the TBC system is. This conclusion is reasonable since the stiffness and the yield strength of the TGO are larger than those of the TC layer.

Fig. 8 demonstrates the variation of the maximum load with the TGO thickness. The maximum load increases with increasing the TGO thickness. The maximum load is 38.37 N for T_{TGO}=0.01 mm, while it is 35.99 N for T_{TGO}=0.0025 mm, which is increased by 6.2% due to the increment of TGO thickness. When the TGO thickness is very small, its effect can be ignored. In order to investigate the effects of the TGO layer, in the following cases, the TGO thickness is taken to be 0.01 mm.

4.3 Influence of the amplitude on indentation response

In order to illustrate the effect of the TGO amplitudes on the residual von Mises equivalent stress after unloading in the indentation test, Fig. 9 gives its distribution for different TGO amplitudes with the thickness of TGO $T_{TGO} = 0.01$ mm and the wavelength $\lambda_{TGO} = 0.06$ mm. This figure clearly shows that the residual stress near

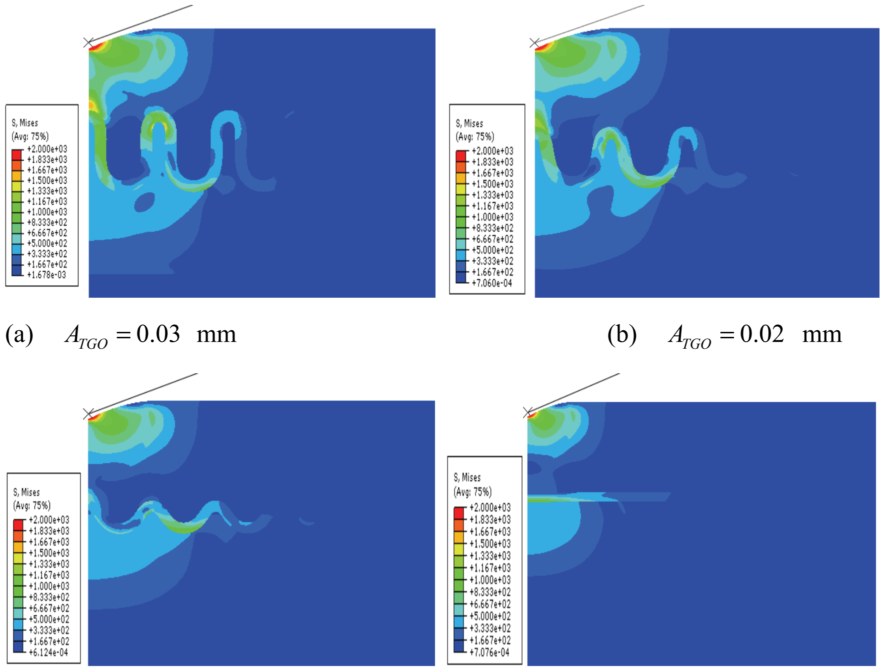

(a) $A_{TGO} = 0.03$ mm (b) $A_{TGO} = 0.02$ mm

(c) $A_{TGO} = 0.01$ mm (d) $A_{TGO} = 0.00$ mm

Figure 9: The distribution of the residual von Mises equivalent stress in TBC for different TGO amplitudes

the indenter is almost unchanged, although the amplitude A_{TGO} varies. However, the residual stress in the TC layer around the wave crest of the TGO adjacent to the indenter decreases as the amplitude A_{TGO} decreases. This is because, as the amplitude of the TGO decreases, the distance between the indenter and the TGO layer increases.

Fig. 10 shows the effect of the amplitudes on the force versus displacement curves of the indentation for the case with$\lambda_{TGO} = 0.06$mm and $T_{TGO} = 0.01$mm. Fig. 11 gives a local enlargement of Fig. 10. As seen, the effect of the amplitudes is obvious since the force versus displacement curves do not overlap when the depth of indentation is beyond 0.01mm (10% of the TC thickness). The load increases as the amplitude increases. The reason is that, when the thickness and wavelength of the TGO layer are kept constant, increasing the amplitude of the TGO layer means

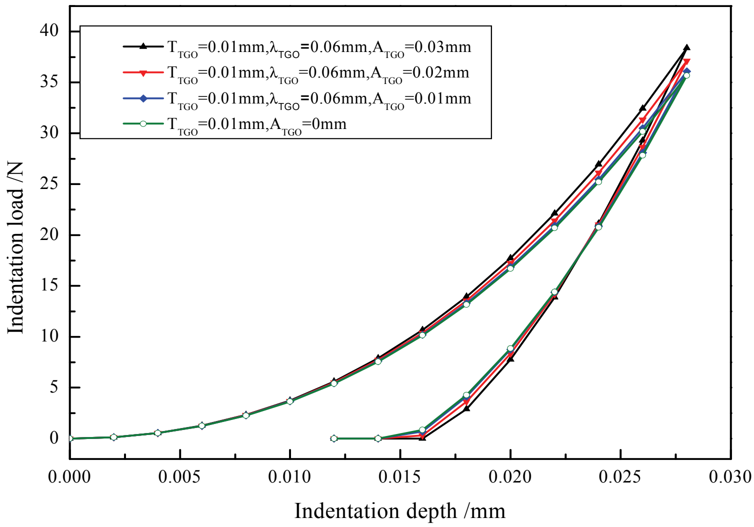

Figure 10: Force versus displacement curves for different amplitudes of TGO

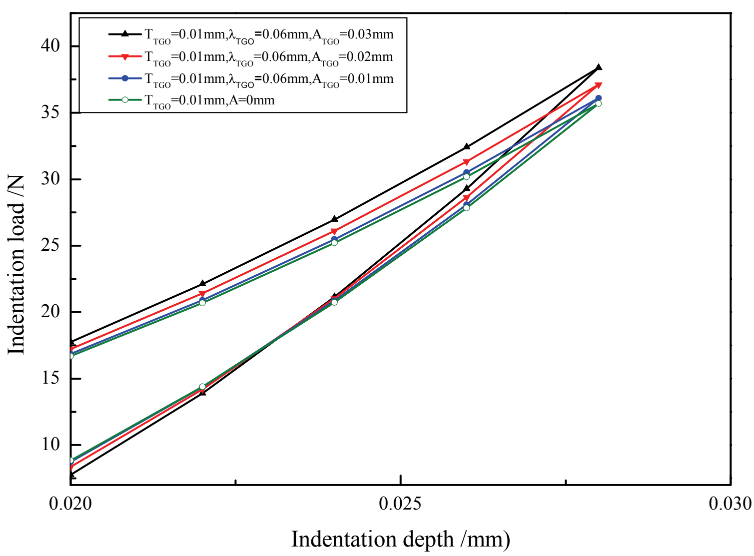

Figure 11: The local enlargement of Fig.10

to increase its volume fraction.

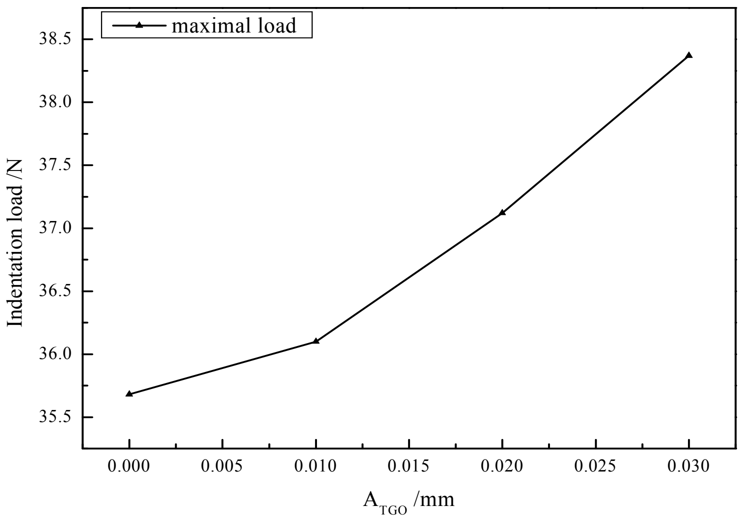

Figure 12: The variation of the maximum load with the amplitude of TGO

Fig. 12 demonstrates the variation of the maximum load of the indentation with the amplitude of TGO. The maximum load increases with increasing the TGO amplitude. The maximum load is 38.37 N as A_{TGO}=0.03mm, while it is 35.68 N as A_{TGO}=0.00mm (plane). The maximum load is increased by 7% due to the increment of TGO amplitude.

4.4 Influence of the wavelength on indentation response

Fig. 13 illustrates the distribution of the residual von Mises equivalent stress after unloading for different wavelength λ_{TGO} with the thickness of TGO $T_{TGO} = 0.01$ mm and the TGO amplitude A_{TGO}=0.03 mm. As seen, in the TC layer the magnitudes of the residual stresses near the indenter are almost same, though the wavelength λ_{TGO} varies. The maximal residual stress in the TC layer appears around the wave crest of the TGO close to the indenter, due to the relatively large stiffness and interface morphology of TGO.

Fig. 14 displays the effect of wavelength on the force versus displacement curves of the indentation for the case with $A_{TGO} = 0.03$ mm and $T_{TGO} = 0.01$ mm. Fig. 15 gives a local enlargement of Fig. 14. As seen, the effect of wavelength is presented since the force versus displacement curves do not overlap when the depth of

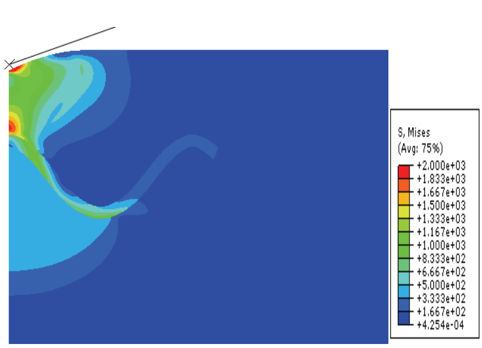

(a) λ_{TGO} =0.15mm

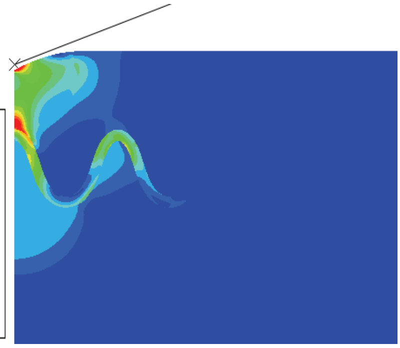

(b) λ_{TGO} =0.1mm

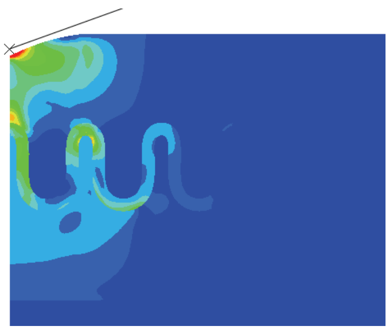

(c) λ_{TGO} =0.06 mm

Figure 13: The distribution of the residual von Mises equivalent stress in TBC for different TGO wavelengths

indentation is greater than 0.01mm (10% of the TC thickness). The load increases as the wavelength decreases. This is due to that, when the thickness and amplitude of the TGO layer are kept constant, decreasing the wavelength of the TGO layer means to increase its volume fraction.

Fig. 16 demonstrates the variation of the maximum load of the indentation with the wavelength of TGO. The maximum load decreases as increasing the TGO wavelength. The maximum load is 38.37 N at λ_{TGO}=0.06 mm, while it is 35.63 N at λ_{TGO}=0.15 mm. The maximum load is decreased by 7.1% due to increasing TGO wavelength.

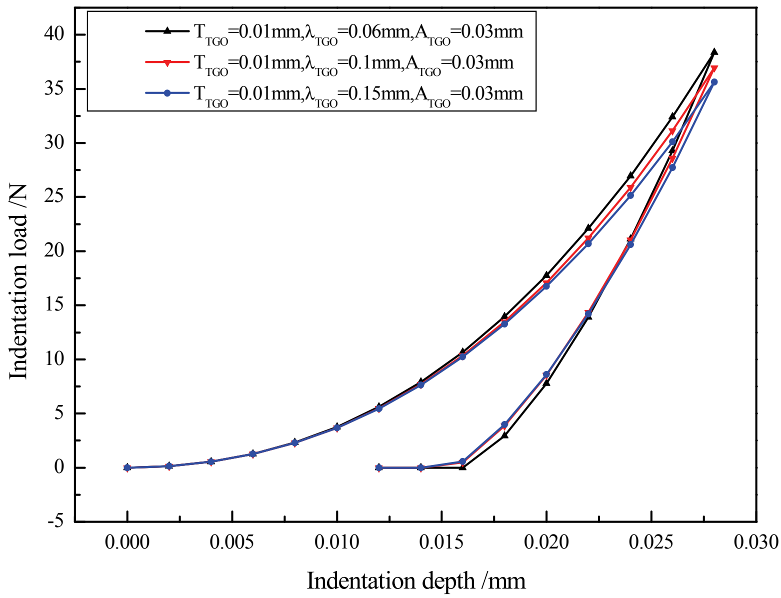

Figure 14: Force versus displacement curves for different wavelength of TGO

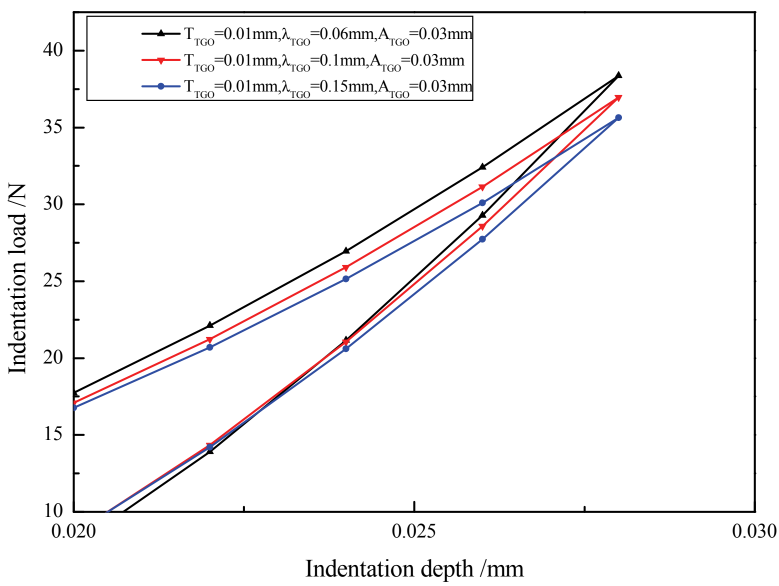

Figure 15: The local enlargement of Fig.14

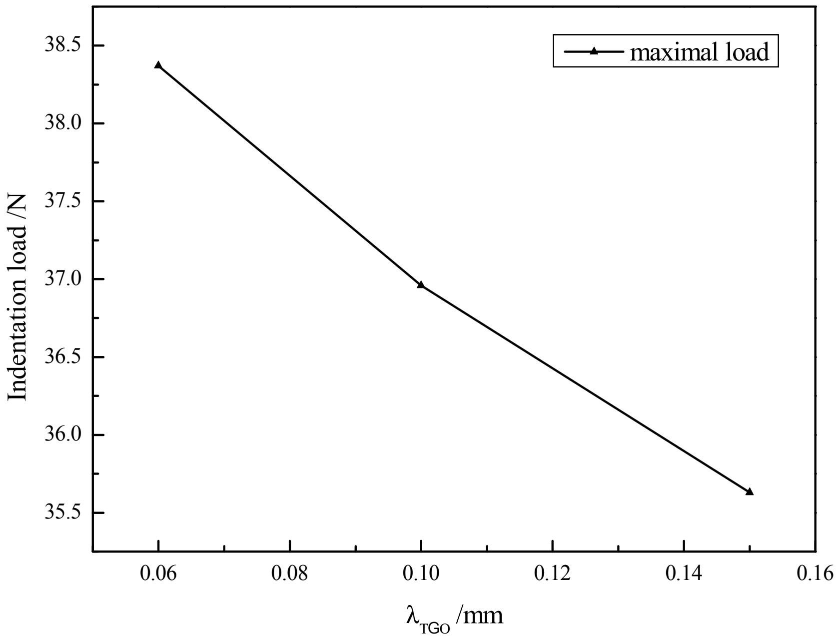

Figure 16: The variation of the maximum load with the wavelength of TGO

5 Conclusions

Based on the finite element analysis, in this paper, an axisymmetric indentation model is employed to analyze the effects of the thermally grown oxide (TGO) roughness on the indentation response of thermal barrier coatings. During operation, the TGO layer becomes thick and rough, then its effects on the indentation response must be considered. The numerical results stated that the amplitude, wavelength, and thickness of the thermally grown oxide layer have significant influences on the indentation response, while the effect of the indenter position can be neglected. The residual stress zones mainly located just below the indenter and around the nearest two peaks of the thermally grown oxide to the indenter. When the indentation displacement is greater than 10% of the thickness of the top coating layer, the influence of TGO roughness on the force versus displacement curves of the indentation must be considered. Correlating this work with the experimental data may lead to improved characterization of the mechanical properties of TBC systems.

Acknowledgement: This work is supported by 973 Program (2007CB707702), NSFC (Grants No. 10672130 and 10972173), and Ministry of Education of China.

References

Aktaa, J., Sfar, K., Munz, D. (2005): Assessment of TBC systems failure mechanisms using a fracture mechanics approach, *Acta Materialia*, Vol. 53, pp. 4399-4413.

Guo, Y.Q., Zhang, K.S., et al. (2006): Effect of substrate performance on the indentation response of coated systems, *Material Engineering*, Vol. 6, pp. 24-27 (in Chinese).

He, M.Y., Hutchinson, J.W., Evans, A.G. (2003): Simulation of stresses and delamination in a plasma-sprayed thermal barrier system upon thermal cycling, *Materials Science and Engineering A*, Vol. 345, pp. 172-178.

Hibbitt, K.S. Inc. (2005): ABAQUS. Pawtucket, RI.

Huang, X., Pelegri, A.A. (2003): Nanoindentation measurements on low-k porous silica thin films spin coated on silicon substrates, *Journal of Engineering Materials and Technology-Transactions of the ASME*, Vol. 125, pp. 361-367.

Huang, X., Pelegri, A.A. (2007): Finite element analysis on nanoindentation with friction contact at the film/substrate interface, *Composites Science and Technology*, Vol. 67, pp. 1311-1319.

Martena, M., Botto, D., Fino, P., et al. (2006): Modelling of TGO system failure: Stress distribution as a function of TGO thickness and thermal expansion mismatch, *Engineering Failure Analysis*, Vol. 13, pp. 409-426.

Nix, W.D. (1989): Mechanical properties of thin films, *Metallurgical Transactions A*, Vol. 20, pp. 2217-2245.

Nix, W.D., Gao, H. (1998): Indentation size effects in crystalline materials: A law for strain gradient plasticity, *Journal of the Mechanics and Physics of Solids*, Vol. 46, pp. 411-425.

Oliver, W.C., Pharr, G.M. (1992): An improved technique for determining hardness and elastic-modulus using load and displacement sensing indentation experiments, *Journal of Materials Research*, Vol. 7, pp. 1564-1583.

Rabiei, A., Evans, A.G. (2000): Failure mechanisms associated with the thermally grown oxide in plasma-sprayed thermal barrier coatings, *Acta Materialia*, Vol. 48, pp. 3963-3976.

Schlichting, K.W., Padture, N.P., Jordan, E.H., et al. (2003): Failure modes in plasma-sprayed thermal barrier coatings, *Mat Sci Eng A*, Vol. 342, pp. 120-130.

Sfar, K., Aktaa, J., Munz, D. (2002): Numerical investigation of residual stress fields and crack behavior in TBC systems, *Materials Science and Engineering A*, Vol. 333, pp. 351-360.

Thompson, J.A., Clyne, T.W. (2001): The effect of heat treatment on the stiffness of zirconia top coats in plasma sprayed TBCs, *Acta Materialia*, Vol. 49, pp. 1565-1575.

Vaidyanathan, K., Jordan, E.H., Gell, M. (2004): Surface geometry and strain energy effects in the failure of a (Ni, Pt)Al/EB-PVD thermal barrier coating, *Acta Materialia*, Vol. 52, pp. 1107-1115.